RSC Advances

PAPER

View Article Online
View Journal | View Issue

Cite this: *RSC Adv.*, 2019, **9**, 5475

A comparative study on atomically precise Au nanoclusters as catalysts for the aldehyde–alkyne–amine (A^3) coupling reaction: ligand effects on the nature of the catalysis and efficiency†

Ying-Zhou Li [ab] and Weng Kee Leong [*a]

Received 4th February 2019
Accepted 6th February 2019

DOI: 10.1039/c9ra00933g

rsc.li/rsc-advances

Atomically precise Au_{13} nanoclusters stabilized by stibines catalyze the aldehyde–alkyne–amine coupling reaction more efficiently than those stabilized by thiols or phosphines. The nature of the catalytic activity is also different, and may be attributed to the weaker coordinating ability of the stibine ligands.

Atomically precise Au nanoclusters have recently emerged as a new class of catalysts for a range of reactions, including the A^3 coupling reaction, which involves a highly efficient assembly, in a single step, of an aldehyde, an amine and an acetylene to form a propargylamine. Propargylamines are valuable precursors to a number of organic heterocyclic substrates, natural products and therapeutic drugs, and have thus found broad applications in synthetic and pharmaceutical chemistry.[1] The A^3 coupling reaction is generally catalyzed by transition metal species, for example, those of Cu, Zn, Rh, Ru, Ir, Ni, Fe, Ag and Au.[2] Among them, noble-metal salts, complexes or nanoparticles, especially those of Au, are found to be more efficient as they can more readily activate the acetylene as the corresponding acetylide.[3] Recently, recyclable Au(0) nanoparticles have been shown to be more efficient than the widely used Au(I) and Au(III) complexes as catalysts for this reaction.[4]

A challenge with the Au nanoparticle catalysts is the establishment of correlations between the particle structure and its catalytic performance, due to the fluidity of the surface structure (coordination pattern between surface metal and ligands).[5] Compared to larger gold nanoparticles, therefore, atomically precise Au nanoclusters with their well-defined molecular structures, make it possible to correlate their surface structures with catalytic performance. The higher surface area to volume associated with their smaller metal core size (<2 nm) also translates to a reduced amount of the catalyst needed. For example, Jin, *et al.*, have reported that the thiolate-protected nanocluster $[Au_{38}(SC_2H_4Ph)_{24}]$ (Au_{38}) could catalyze the A^3 coupling reaction, and the high catalytic efficiency was ascribed to the synergistic effect between the electron-rich Au core and the electron-deficient surface of the nanoclusters.[6] The group of Obora reported the use of the thiolate-protected nanocluster $[Au_{25}(SC_2H_4Ph)_{18}][TOA]$ (Au_{25}, TOA = tetraoctylammonium) as an efficient catalyst for the reaction and they believed that the surface Au atoms, sterically unblocked by the thiolate ligands, served as active sites in the catalytic process,[7] and Li, *et al.*, reported that the reaction could also be catalyzed by supported Au nanoparticles derived from $[Au_{25}(PPh_3)_{10}(C{\equiv}CPh)_5]X_2$ (Au'_{25}, X = Cl or Br), which has phosphine and alkyne as protecting ligands. It was demonstrated in the latter that removal of one phosphine ligand from the supported Au'_{25} cluster was necessary to enable catalysis.[8] Finally, Wu, *et al.*, reported an Au–Cd nanocluster, $[Au_{13}Cd_2(PPh_3)_6(SC_2H_4Ph)_6(NO_3)_2]_2Cd(NO_3)_4$ ($Au_{26}Cd_4$), with high catalytic activity which was ascribed to the cooperative effect between the peripheral Cd and adjacent Au atoms on the surface of the Au_{13} icosahedral core.[9]

It is clear from the foregoing that the surface structure of the Au nanocluster, including the ligand binding strength, may have a significant influence on the catalytic performance. In this regard, Au nanoclusters protected by more labile ligands may be expected to be more efficient catalysts. We have recently reported the preparation of an Au_{13} nanocluster stabilized by stibine ligands, *viz.*, $[Au_{13}\{Sb(p\text{-tolyl})_3\}_8Cl_4][Cl]$ (Au_{13}).[10] We anticipated that it may catalyze the A^3 coupling reaction more readily than the previously reported phosphine- and thiolate-protected clusters $[Au_{11}(PPh_3)_8Cl_2][Cl]$ (Au_{11}),[11] and Au_{25};[12] the weaker bond between the Au_{13} core and stibine ligands should lead to more ready ligand dissociation to expose catalytically active Au sites.

The thermogravimetric analysis (TGA) curves for crystalline Au_{25}, Au_{11} and Au_{13} show that weight loss at 300 °C is *ca.* 37, 50 and 56%, respectively (Fig. 1), matching the theoretical values (37, 50 and 57%, respectively) corresponding to loss of all coordinating ligands. While the loss for Au_{13} begins at *ca.* 145 °C, that for Au_{11} and Au_{25} begin at *ca.* 165 °C and 195 °C,

[a]*Division of Chemistry & Biological Chemistry, Nanyang Technological University, 21 Nanyang Link, 637371, Singapore. E-mail: chmlwk@ntu.edu.sg*

[b]*Shandong Provincial Key Laboratory of Molecular Engineering, Qilu University of Technology (Shandong Academy of Science), Ji'nan, 250353, People's Republic of China*

† Electronic supplementary information (ESI) available: Experimental, ^1H NMR spectra, UV-Vis spectra and plots of conversion *vs.* time for the A^3 coupling reaction. See DOI: 10.1039/c9ra00933g

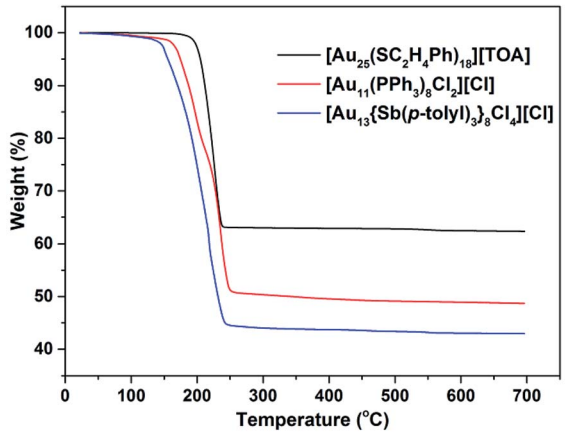

Fig. 1 TGA curves for Au_{25}, Au_{13} and Au_{11}.

respectively, clearly demonstrating that the stibine-protected nanocluster is thermally less stable than the phosphine- and thiolate-protected ones.

A comparative study was carried out for the A^3-coupling reaction of phenylacetylene, piperidine and benzaldehyde with Au_{38}, Au_{25}, Au'_{25} and $Au_{26}Cd_4$ as catalysts (Table 1). The first three of these, *viz.*, Au_{38}, Au_{25} and Au'_{25}, have already been reported to be efficient catalysts for the reaction at very low catalyst loadings (0.30–0.38 mol% based on Au atoms) but at elevated reaction temperatures (80–100 °C) (entries 2–4); $Au_{26}Cd_4$ catalyzed the reaction at room temperature but with a higher catalyst loading (13 mol% based on Au atoms) (entry 5). Although a straightforward comparison of those results is difficult as they were carried out under different reaction conditions, some general observations include: (1) the reaction with Au nanoclusters as catalysts gave a higher yield when carried out neat or in water (entries 1–3). This is consistent with previous reports that water was beneficial with Au(I) salts as catalysts.[13] (2) It has been suggested that elevated reaction temperatures were required as it favoured formation of the cationic imine intermediate, and facilitated catalyst activation *via* removal of the protecting ligands (entry 4). (3) An inert

Table 1 A^3 coupling reaction of benzaldehyde, piperidine, and phenylacetylene with Au nanoclusters as catalysts[a]

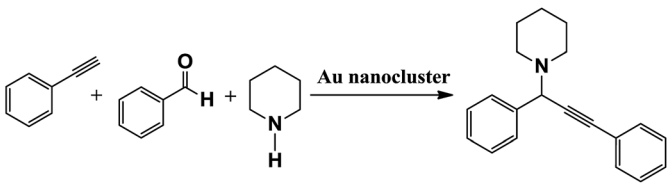

Entry	Cat.[b]	Cat. loading[c] (mol%)	Time (h)	Sol.	T (°C)	Conv.[d] (%)	Ref.
1[e]	Au_{25}	0.10	24	Tol	80	89[f]	7
2	Au_{25}	0.013	5	None	80	~95%[g]	6
3	Au_{38}/CeO_2	0.010	5	None	80	99	
		0.010	5	H_2O	80	94	
		0.010	5	Tol	80	80	
4	Au'_{25}/TiO_2	0.012	18	H_2O	80	66	8
		0.012	18	H_2O	100	90	
5	$Au_{26}Cd_4$	0.50	5	DCM	r.t.	80[f]	9
Entries below are from this work							
6	Au_{25}	0.50	12	DCM[h]	21	0	—
7	Au_{11}	0.50	12	DCM[h]	21	0	—
8	Au_{13}	0.50	24	DCM	21	47	—
9	Au_{13}	0.50	19	$CHCl_3$	21	25	—
10	Au_{13}	0.50	12	None	21	79	—
11	Au_{25}	0.50	12	None	21	4	—
12	Au_{11}	0.50	12	None	21	Trace	—
13	Au_{13}	0.03	15	None	21	32	—
14	Au_{25}	0.03	15	None	21	0	—
15	Au_{11}	0.03	15	None	21	0	—
16	Au_{13}	0.03	5	None	50	81	—
			12	None	50	92	—
17	Au_{25}	0.03	5	None	50	7	—
			12	None	50	69	—
18	Au_{11}	0.03	12	None	50	Trace	—

[a] Benzaldehyde (1.0 mmol), piperidine (1.2 mmol), phenylacetylene (1.3 mmol), solvent (1.0 ml, if present). [b] Supported catalysts are at 1 wt%, *i.e.*, 1 mg of Au nanocluster on 100 mg of support. [c] Based on Au nanoclusters, with respect to amount of benzaldehyde. [d] Conversion of benzaldehyde, determined by ^{1}H NMR. [e] Different reactant ratios used: benzaldehyde (0.5 mmol), piperidine (1.0 mmol), phenylacetylene (1.5 mmol). [f] Isolated yields. [g] Conversion not given in original report; estimated from ^{1}H NMR plot provided in ESI. [h] Three other solvents were also tested: DCE, $CDCl_3$ and toluene.

atmosphere was needed in order to avoid rapid oxidation of the substrates exacerbated by the elevated temperature. From the economic and environmental perspectives, therefore, an efficient catalyst which can catalyze the A^3 coupling reaction under ambient conditions, without an organic solvent (neat), and in air, would be desirable.

In this work, we have found that Au_{25} and Au_{11} (0.5 mol%) failed to afford any product at room temperature (21 °C), under aerobic conditions, in any of the organic solvents tested (dichloromethane (DCM), 1,2-dichloroethane (DCE), chloroform ($CHCl_3$) or toluene (Tol)) (entries 6, 7) even after 12 h. Another previously reported icosahedral cluster $Au_{13}(PPh_3)_4(SC_2H_4Ph)_4$ also showed no catalytic activity under similar reaction conditions.[9] In contrast, Au_{13} gave the desired product under the same reaction conditions, albeit at a relatively low conversion of benzaldehyde: 47% in DCM after 24 h, and 25% in $CHCl_3$ after 19 h (entries 8, 9). These figures were obtained by monitoring the reactions in CD_2Cl_2 and $CDCl_3$ by ^{1}H NMR spectroscopy (Fig. S1–S4†). The lack of activity in the thiolate and phosphine-stabilised nanoclusters is probably related to the lack of catalytically active sites at room temperature since these ligands are more strongly bound.

The neat reactions (all the three reactants are liquids at room temperature) showed obvious improvement for Au_{13}, with the conversion rate reaching 79% after 12 h (entry 10), and ~90% with prolonged reaction time (36 h). This can be ascribed to good solubility of the catalyst, and the higher substrate concentrations. The reaction kinetics monitored through ^{1}H NMR spectroscopy (Fig. S5†), showed that conversion to propargylamine rapidly increased to 57% in the first 5 h and further to >90% over a prolonged reaction time (Fig. 2). Fitting the data for the first 10 h to first-order reaction kinetics gave a rate constant $k = 0.14\ h^{-1}$ (Fig. S6†). The turnover frequency (TOFs) at 6 min (2.9% conversion), was estimated to be 58 h^{-1} per Au_{13} cluster or 4.5 h^{-1} per Au atom. Both Au_{25} and Au_{11} showed very low conversion at 12 h of reaction under the same conditions (0.5 mol% catalyst loading, neat) (Table 1, entries 11 and 12). More significantly, both catalysts showed an induction period (~12 h and 50 h, respectively), suggesting that the active species was not Au_{25} or Au_{11} (Fig. 2). As may be expected, lowering the catalyst loading to 0.03 mol% led to a significant drop in conversion rates (entries 13–15), and increasing the temperature to 50 °C had a dramatic effect on the conversion for Au_{13} and Au_{25} but not Au_{11} (entries 16–18). At 50 °C, the reaction with Au_{25} was still within the induction period for the first 5 h. A comparison of the performance of Au_{13} with Au_{25} at the 5 h mark showed that the former (81% conversion, TON = 208 per Au atom) outperformed the latter (7% conversion, TON = 9.3 per Au atom) (Fig. S20 and S21†).

It is known that the active catalyst in many reactions catalyzed by Au salts or complexes are actually Au(0) nanoparticles, or other Au clusters formed during the reaction; these generally exhibit an induction period during which the catalytically active species is formed, at a slower rate than for the product-formation reaction.[14] In the case of Au_{13} here, no induction period was observed (Fig. 2). Since the induction period is related to the concentration of the precursor to the active catalyst, it is also possible that there may have been a short induction period. To rule this out, the reaction was repeated with a lower catalyst loading of 0.03 mol%; although the conversion rate was decreased significantly (32% conversion after 15 h, entry 13), an induction period was still not observed (Fig. S8†). In all these reactions, there were no obvious signs of nanoparticle formation or precipitation. The catalyst could be recovered from the room temperature reaction by precipitation with hexane (after 60 h, at 93% conversion), and the UV-Vis spectrum of the recovered catalyst showed the characteristic absorption peaks of Au_{13} and some decomposition, although we have not been able to determine the identity of the decomposition products (Fig. S7†). Monitoring of the reaction by ^{1}H NMR spectroscopy also showed that Au_{13}, or a structural analogue (a "less intact" Au_{13}), was present throughout the reaction; there were no obvious change in intensity or position of the resonances (Fig. S9†). In addition, we have also found that although $(p\text{-tolyl})_3SbAuCl$, the most likely dissociated fragment from Au_{13}, could catalyze the reaction it had a much lower efficiency (Fig. S10†). Taken together, these results suggest that the catalytically active species is most likely Au_{13}, or a "less intact" Au_{13} nanocluster in which one or more ligands have dissociated or been replaced. Thus Au_{13} behaves as a homogeneous, or what has been termed as quasi-homogeneous, catalyst,[15] and its higher catalytic activity may be attributed to the weaker coordination of the stibine ligands to the Au_{13} core.

For Au_{25}, monitoring the reaction by UV-Vis spectroscopy showed that it gradually decomposed during reaction, as reflected by the replacement of its characteristic peak at *ca.* 670 nm by another at *ca.* 840 nm (Fig. 3). The absence of a surface plasmonic resonance (SPR) peak suggests that little or no larger Au(0) nanoparticles (>4 nm) were formed.[16] Monitoring the same reaction by ^{1}H NMR spectroscopy showed that the Au_{25} gradually disappeared after the induction period, accompanied by an obvious increase in the conversion (Fig. S11†). The oxidative decomposition of Au_{25} to generate some Au(I) species during the catalysis of styrene oxidation has already been noted previously.[17] Together with the results here, we propose that Au_{25} is not the active catalyst for the A^3 coupling reaction, at least under the given reaction conditions here. Instead, in the presence of air, there is decomposition into the active catalyst which is probably a mixture of smaller Au clusters.

Similarly, the much lower catalytic efficiency for Au_{11} may be partly attributed to its conversion to neutral $Au_{11}(PPh_3)_7Cl_3$ (Au'_{11}) which is poorly soluble in the reaction mixture and precipitated out, leading to a much lower precursor catalyst concentration; the orange Au'_{11} could be collected by washing with hexane and was identified by its ^{1}H NMR spectrum (Fig. S12 and S13†).[11] Just as in the case of Au_{25}, no SPR peak was observed in the UV-Vis spectrum throughout the reaction (Fig. S14, S15 and S18†). That the catalytic activity of Ph_3PAuCl, albeit at a lower catalyst loading based on Au atoms, was observed to be better in comparison initially, may be attributed to the absence of an induction period (Fig. S16†), and suggests that the catalytically active species are smaller Au clusters

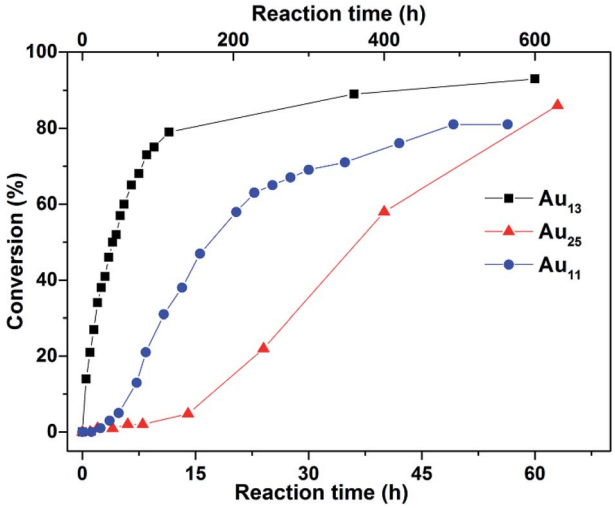

Fig. 2 Conversion (%) of benzaldehyde as a function of reaction time (h) catalysed by the various gold nanoclusters. Timescale at the top is for Au_{11} and that at the bottom is for Au_{13} and Au_{25}.

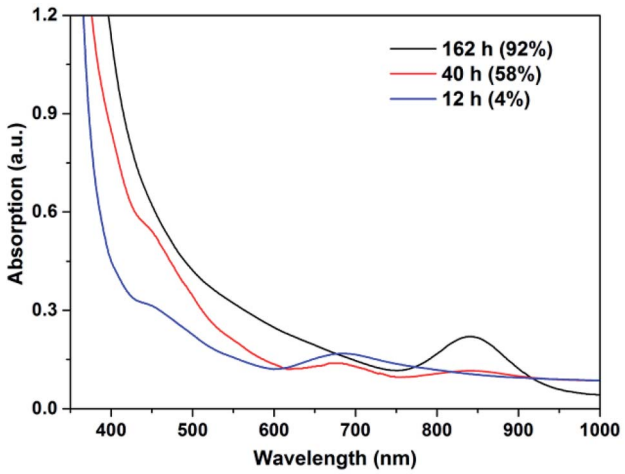

Fig. 3 Electronic spectra of the crudes catalyzed by Au_{25} (0.5 mol%) in neat conditions at 21 °C. The percentages in parentheses are the corresponding conversion of benzaldehyde.

formed through decomposition of Au_{11} and/or Au'_{11}. Monitoring the A^3 coupling reaction with Au_{11} showed that while the nanocluster was more soluble at 50 °C, it also decomposed to other unknown species as conversion increased (Fig. S17†); the UV-Vis spectrum of the crude at 80% conversion showed no distinct absorption peak, indicating almost complete decomposition of Au_{11} and Au'_{11} (Fig. S18†). Consistent with all these is the observation that initial heating of the reaction mixture at 50 °C for 12 h significantly diminished the induction period (Fig. S19†). That Au_{11} nanoclusters can act as catalyst precursors has also been reported previously.[18]

In conclusion, we have found that the stibine-protected nanocluster Au_{13} was a more efficient catalyst than the thiolate- and phosphine-protected nanoclusters for the aldehyde–acetylene–amine (A^3) coupling reaction. The reaction proceeded under mild reaction conditions and in air. In contrast to the thiolate- and phosphine-protected nanoclusters, the stibine-protected nanocluster behaved as a homogeneous or quasi-homogeneous catalyst. The effect of the ligand on catalytic performance for Au nanoclusters has implications for the design and preparation of more catalytically active Au nanoclusters. Studies into this and with a wider substrate scope are currently underway.

Conflicts of interest

There are no conflicts to declare.

Acknowledgements

This work was supported by a research grant (SERC grant no. 1521200076) from the Agency for Science, Technology and Research (A*STAR), Singapore.

Notes and references

1 (*a*) J. L. Wright, T. F. Gregory, S. R. Kesten, P. A. Boxer, K. A. Serpa, L. T. Meltzer, L. D. Wise, S. A. Espitia, C. S. Konkoy, E. R. Whittemore and R. M. Woodward, *J. Med. Chem.*, 2000, **43**, 3408–3419; (*b*) K. K.-Y. Kung, G. L. Li, L. Zou, H.-C. Chong, Y.-C. Leung, K.-H. Wong, V. K.-Y. Lo, C.-M. Che and M.-K. Wong, *Org. Biomol. Chem.*, 2012, **10**, 925–930; (*c*) N. Uhlig and C. J. Li, *Org. Lett.*, 2012, **14**, 3000–3003; (*d*) A. Renhack, T. Jumpertz, J. Ness, S. Baches, C. U. Pietrzik, S. Weggen and B. Bulic, *Bioorg. Med. Chem.*, 2012, **20**, 6523–6532.

2 (*a*) V. A. Peshkov, O. P. Pereshivko and E. V. Van der Eycken, *Chem. Soc. Rev.*, 2012, **41**, 3790–3807; (*b*) K. Lauder, A. Toscani, N. Scalacci and D. Castagnolo, *Chem. Rev.*, 2017, **117**, 14091–14200.

3 R. Skouta and C.-J. Li, Gold-Catalyzed Multi-Component Reactions, in *Gold Catalysis*, Imperial College Press, 2014, pp. 225–251.

4 (*a*) M. Kidwai, V. Bansal, A. Kumar and S. Mozumdar, *Green Chem.*, 2007, **9**, 742–745; (*b*) K. K. R. Datta, B. V. S. Reddy, K. Ariga and A. Vinu, *Angew. Chem., Int. Ed.*, 2010, **49**, 5961–5965; (*c*) B. Karimi, M. Gholinejad and M. Khorasani, *Chem. Commun.*, 2012, **48**, 8961–8963; (*d*) B. J. Borah, S. J. Borah, K. Saikia and D. K. Dutta, *Catal. Sci. Technol.*, 2014, **4**, 4001–4009.

5 R. Jin, C. Zeng, M. Zhou and Y. Chen, *Chem. Rev.*, 2016, **116**, 10346–10413.

6 Q. Li, A. Das, S. Wang, Y. Chen and R. Jin, *Chem. Commun.*, 2016, **52**, 14298–14301.

7 Y. Adachi, H. Kawasaki, T. Nagata and Y. Obora, *Chem. Lett.*, 2016, **45**, 1457–1459.

8 Y. Chen, C. Liu, H. Abroshan, Z. Li, J. Wang, G. Li and M. Haruta, *J. Catal.*, 2016, **340**, 287–294.

9 M.-B. Li, S.-K. Tian and Z. Wu, *Chin. J. Chem.*, 2017, **35**, 567–571.

10 Y.-Z. Li, R. Ganguly, K. Y. Hong, Y. Li, M. E. Tessensohn, R. Webster and W. K. Leong, *Chem. Sci.*, 2018, **9**, 8723–8730.

11 L. C. McKenzie, T. O. Zaikova and J. E. Hutchison, *J. Am. Chem. Soc.*, 2014, **136**, 13426–13435.
12 M. Zhu, E. Lanni, N. Garg, M. E. Bier and R. Jin, *J. Am. Chem. Soc.*, 2008, **130**, 1138–1139.
13 C. Wei and C.-J. Li, *J. Am. Chem. Soc.*, 2003, **125**, 9584–9585.
14 (*a*) J. Oliver-Meseguer, J. R. Cabrero-Antonino, I. Domínguez, A. Leyva-Pérez and A. Corma, *Science*, 2012, **338**, 1452–1455; (*b*) G. A. Price, A. K. Brisdon, S. Randall, E. Lewis, D. M. Whittaker, R. G. Pritchard, C. A. Muryn, K. R. Flower and P. Quayle, *J. Organomet. Chem.*, 2017, **846**, 251–262.
15 R. R. Nasaruddin, T. Chen, N. Yan and J. Xie, *Coord. Chem. Rev.*, 2018, **368**, 60–79.
16 G. Ramakrishna, O. Varnavski, J. Kim, D. Lee and T. Goodson, *J. Am. Chem. Soc.*, 2008, **130**, 5032–5033.
17 T. A. Dreier, O. Andrea Wong and C. J. Ackerson, *Chem. Commun.*, 2015, **51**, 1240–1243.
18 E. S. Andreiadis, M. R. Vitale, N. Mézailles, X. Le Goff, P. Le Floch, P. Y. Toullec and V. Michelet, *Dalton Trans.*, 2010, **39**, 10608–10616.